Preliminary simulation study of the front-end electronics for the central detector PMTs

A. F. Barbosa
Centro Brasileiro de Pesquisas Fsicas - CBPF, e-mail: laudo@cbpf.br

Abstract

A preliminary study on the design of the front-end pre-amplifier for the central detector photomultipliers (PMTs) of the Angra Neutrino project is presented. The study is based on PSPice simulations, relying on models of two operational amplifiers provided by the manufacturers. An integrating stage is implemented, followed by a gain stage and filtering that should prepare signals with amplitude ranging within $\pm 1V$, and time development compatible with an analog-to-digital converter (ADC) featuring a sampling period close to $10ns$.

1 Introduction

The Angra anti-neutrino detector [1] is expected to be composed by two main detecting systems. The central one includes three cylindrical liquid volumes of detecting media, surrounded by approximately 100 PMTs. The outer system is intended to implement a veto for cosmic rays and other events not related to the anti-neutrinos produced by the nuclear reactor [2]. Hamamatsu model R5912 PMTs are presently under consideration to be used in the central detector. The shape of the signal output in this PMT is shown in Figure 1. By illuminating the PMT with very narrow and low amplitude LED light

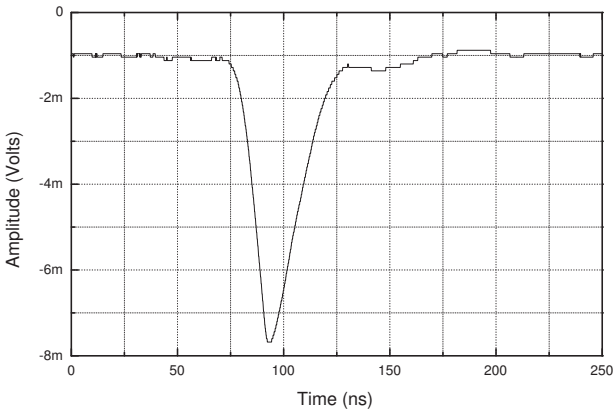

Figure 1: High amplitude averaged signal captured for photoelectrons in one R5912 PMT, operating at gain 10^7.

pulses, it has been possible to observe signals from individual photoelectrons directly from a digital oscilloscope [3]. The data acquisition was triggered by a prompt signal from the LED pulse generator. The result is shown in Figure 2. It may be seen from Figures 1 and 2 that the signals with which we

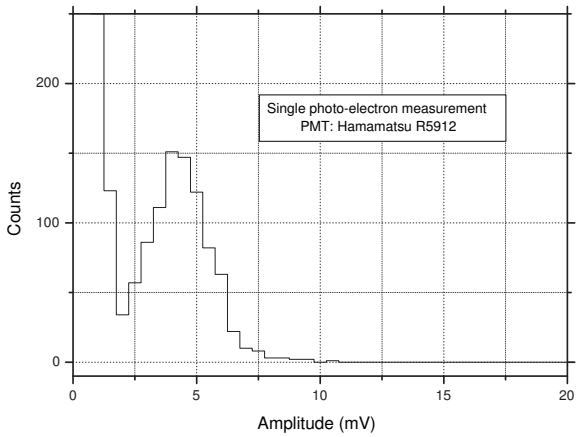

Figure 2: Single photoelectrons measurement, PMT operating at gain 10^7.

have to deal in the anti-neutrino detector are relatively fast ($\approx 20ns$ rise-time), with amplitudes close

to the noise level. The scope of the present note is to start a study on the strategy to convert these signals into a shape that can be analyzed by an ADC operating at a conversion rate around $100MHz$. Two operational amplifiers have been chosen to be the basic elements of the amplifying and shaping circuit: $OPA657$ and $AD9617$ (in the following referred to as circuits #1 and #2, respectively). The performance of each circuit stage has been simulated for the two operational amplifiers. In the next sections we show the results related to each of them, and the final version of the complete circuit that has been obtained.

2 The Integration Stage

The standard configuration for an integrating circuit using operational amplifiers is shown in Figure 3. The essential circuit elements are the input resistor R_1 and the feed-back capacitor C_f. The resistor

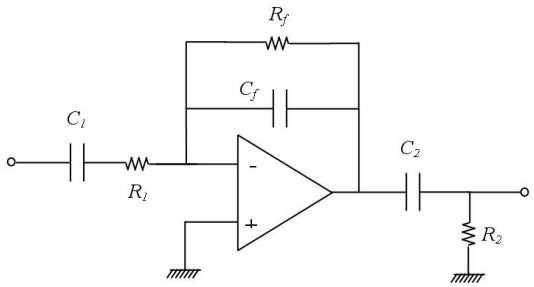

Figure 3: The basic integrating circuit using an operational amplifier.

R_f in the feed-back network is present only to provide a path for discharging the capacitor C_f, but it has an effect on the signal shape, as will be shown in the next subsection. Capacitors C_1 and C_2 isolate the integrating stage from DC coupling to the previous and to the next stages. Their capacitances are supposed to be high enough not to interfere with the integration operation. Resistor R_2 represents the loading effect of the next circuit stage. Under these assumptions, it may be shown that the relation between the input (v_{in}) and the output (v_{out}) signals is given by:

$$v_{out} = -\frac{1}{R_1 C_f}\int v_{in}dt \tag{1}$$

We see that the output signal is numerically equivalent in amplitude to the integral of the input signal. In addition, the output is inverted with respect to the input and multiplied by a number ($\frac{1}{R_1 C_f}$), which may be used to set an amplification or attenuation factor. The component values used in the simulation of the integrating stage with the operational amplifiers #1 and #2 are shown in Table 1 below. With this choice of components, the circuit response to an input pulse very similar in its time development to the average PMT output signal has proven to be in good agreement with Eq. 1. This is clearly seen in Figures 4 and 5.

On the plots in Figures 4 and 5 the time constant R_1C_f is referred to as *RC*. The input pulse is triangular in shape, with $20ns$ rise and fall times, $1mV$ amplitude. Its integral is therefore $20ns \times 1mV$. The simulated time constants were such that the output signal amplitude was set to 100%, 75%, 50% and 25% of the input amplitude. We notice from Table 1 that, due to the specific architecture of the operational amplifiers #1 and #2, the particular values for *R* and *C* are different, although the time

#1	#2
$C_1 = C_2 = 0.1\mu F$	$C_1 = C_2 = 0.1\mu F$
$C_f = 10pF$	$C_f = 1nF$
$R_1 = (2, 2.66, 4, 8)K\Omega$	$R_1 = (20, 26.6, 40, 80)\Omega$
$R_f = 10M\Omega$	$R_f = 100K\Omega$
$R_2 = 1K\Omega$	$R_2 = 1K\Omega$

Table 1: Component values for the integrating stage

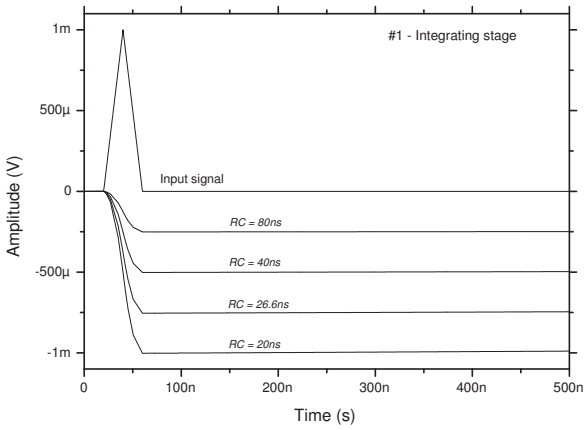

Figure 4: The integration stage output for circuit #1.

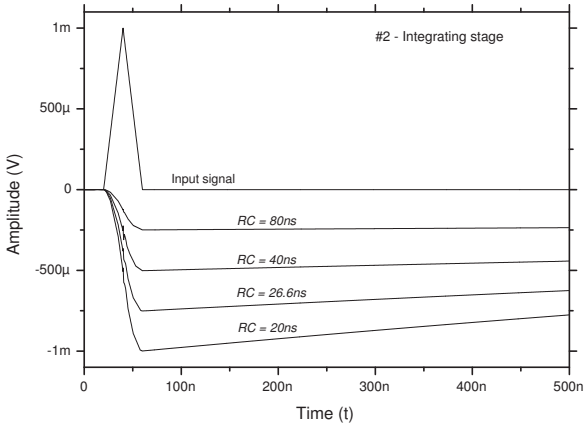

Figure 5: The integration stage output for circuit #2.

constants are the same. It also has to be noticed that we took an input pulse a bit faster than what is seen in Figure 1, because the digital oscilloscope in which the PMT pulses were observed is limited in bandwidth to $100MHz$. The actual pulses from the PMT may therefore be faster, so we took faster pulses in the simulation. Given the oscilloscope bandwidth and the shape of the observed signal, we

estimate that a factor ≈2 in the rise and fall times, with respect to the observed signal, is realistic.

2.1 The effects of the loading and feed-back resistors

The effect of the loading resistor is basically the result of the differentiating circuit that it establishes with capacitor C_2. It is also determined by the driving capability of the operational amplifier. The overall effect for circuits #1 and #2 are shown respectively in Figures 6 and 7. Three values of the loading resistor were simulated: 1KΩ, 50Ω, 1Ω. The integrating time constant, R_1C_f, was kept at the required value to provide 100% output amplitude, as mentioned above. The feed-back resistor, R_f,

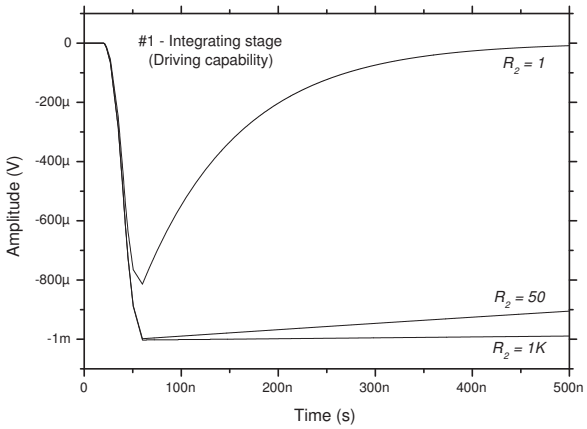

Figure 6: Driving capability for circuit #1 under different loading resistors.

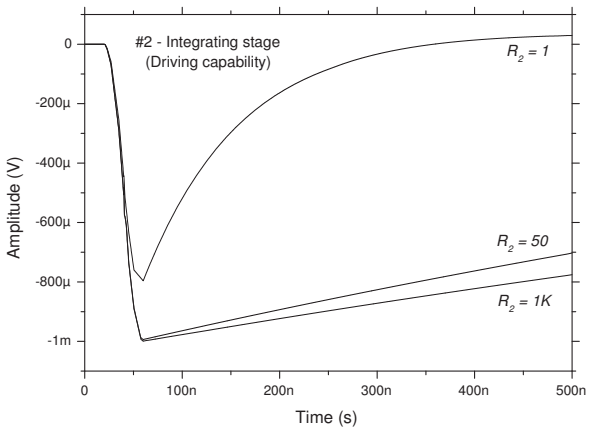

Figure 7: Driving capability for circuit #2 under different loading resistors.

provides a path for discharging capacitor C_f. If R_f was not present, there would remain a DC level at the output for every integrated pulse, and this would define a pedestal on top of which other integrated

events would pile up and soon saturate the operational amplifier. There is, therefore, another time constant defined by the product $R_f C_f$, that shapes the output signal, bringing the pedestal back to the ground level. By keeping the loading resistor fixed at 1KΩ, we varied the R_f value, so that the shape of the output signal could be evaluated. The results are shown in Figures 8 and 9. The C_f capacitor was $10pF$ for circuit #1 and $1nF$ for circuit #2.

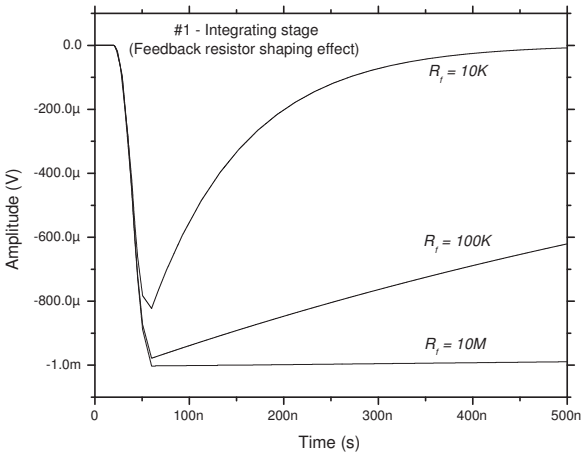

Figure 8: $R_f C_f$ effect for circuit #1, with R_2=1KΩ.

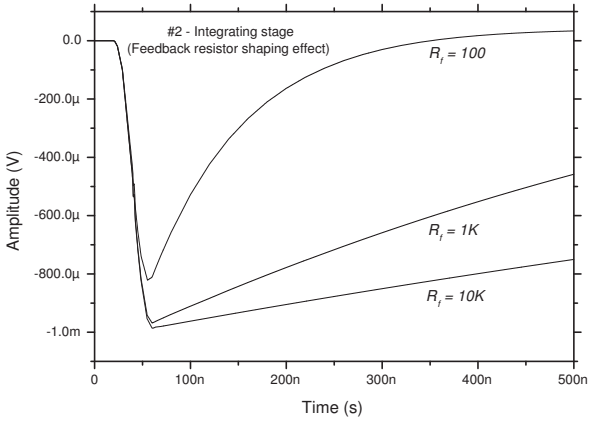

Figure 9: $R_f C_f$ effect for circuit #2, with R_2=1KΩ.

3 The Amplifying Stage

As mentioned above, the PMT pulses are supposed to be analyzed by an analog-to-digital conversion chain, with sampling rate close to $100MHz$ and input range $\pm 1V$. The PMT and the pre-amplifier

gains have to be set according to the expected average number of photoelectrons *per* PMT *per* event. This information will emerge from precise detector simulations which are now being undertaken for the Angra case [4], but are not yet concluded. Let us suppose, as a most-difficult case scenario, that the pre-amplifier should provide a half-scale ($1V$) pulse amplitude for a single photo-electron, with the PMT operating at the same conditions as those that produced the spectrum shown in Figure 2. We see that a gain factor close to 250 would be required. Since we are using operational amplifiers as the main circuit units, we may simply configure them as amplifying blocks following the integration stage. This approach has been tested in the simulation. Figure 10 is a summary of the results. For

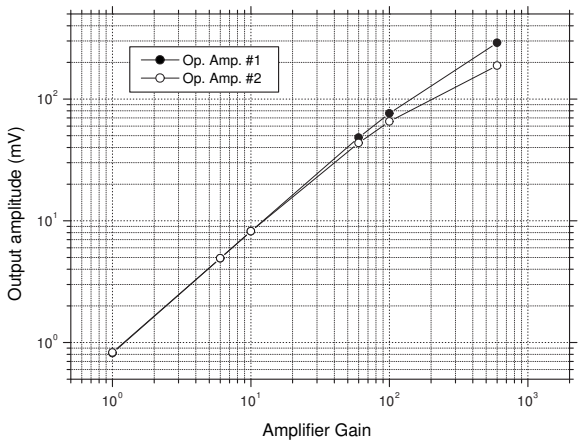

Figure 10: Non-linearity due to the gain×bandwidth limit for circuits #1 and #2.

the simulation referred to in this Figure, a non-inverting amplifier block was added to the integrating stage. The input pulse is the same previously used. We see that the linearity relation between the input and the output amplitudes, as the gain increases, is gradually lost for gain factors above a few times 10. Circuit #1 features a better performance, but both #1 and #2 clearly fail to be linear for gains above 100. This behavior is expected from the parameters announced by the manufacturers, especially the gain×bandwidth product. In short, high gain implies limited bandwidth, so that part of the spectral components of the input signal are not amplified and the waveform is distorted. This is seen in Figure 11, where the input and output pulses are shown for implemented gain 600. The effective gain obtained is below 300. In Figure 11, the top and and the middle plots show the signal at the input of the amplifying block for circuits #1 (with $C_f = 10pF, R_f = 10K\Omega, R_1 = 2K\Omega, R_2 = 1K\Omega$) and #2 ($C_f = 1nF, R_f = 100\Omega, R_1 = 20\Omega, R_2 = 1K\Omega$), respectively. In the bottom plot, the output signal for both circuits is shown.

3.1 Improving the gain by acting on the integrating stage

Although, according to the data in Figure 11, an effective gain close to the required (250) is obtained by setting the amplifying stage gain to 600, this solution is of course not ideal. In addition to the distortion due to the limited bandwidth, we also have to take into account that the frequencies within the bandwidth are amplified by the factor 600. The spectral components of the signal and of the electronic noise lying inside the bandwidth are amplified with gain 600, while the signal

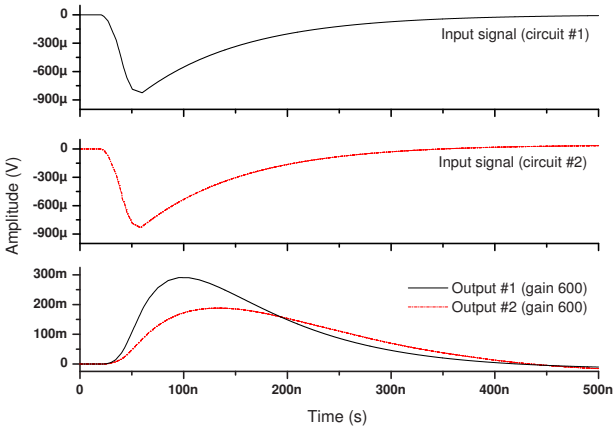

Figure 11: Output waveform distortion due to gain non-linearity.

higher frequency spectral components are amplified with a lower gain factor. The output is therefore prone to be noisy. As an alternative, we may act at the level of the integrating stage and choose a lower R_1C_f product, so that a higher output amplitude is obtained, according to Eq. 1. By doing this, we may alleviate the gain factor at the gain stage. As an example, we show in Figure 12 the output signal shape for the amplifying stage operating with gain 60. The data in Figure 12 refer

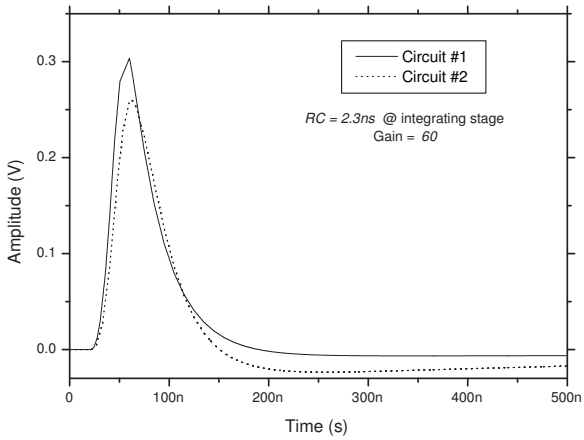

Figure 12: Correction for non-linearities, obtained by reducing the gain and the integration stage time constant.

to a case where we have: $C_f = 3.3pF, R_f = 10K\Omega, R_1 = 700\Omega, R_2 = 1K\Omega$ in circuit #1 and $C_f = 330pF, R_f = 10K\Omega, R_1 = 7\Omega, R_2 = 1K\Omega$ in circuit #2. The same effective gain of Figure 11 is obtained, with the amplifying stage operating at a ten times lower gain. We see that the distortion at the fast rising edge of the signal is well suppressed for both circuits #1 and #2.

#1	#2
$C_1 = 0.1\mu F$	$C_1 = 0.1\mu F$
$C_2 = C_3 = 1\mu F$	$C_2 = C_3 = 1\mu F$
$C_{out} = 10pF$	$C_{out} = 10pF$
$C_f = 4.7pF$	$C_f = 15pF$
$R_1 = 200\Omega$	$R_1 = 20\Omega$
$R_f = 10K\Omega$	$R_f = 700\Omega$
$R_2 = 1K\Omega$	$R_2 = 1K\Omega$
$R_3 = 50$	$R_3 = 50$
$R_g = 3K\Omega$	$R_g = 3K\Omega$
$R_4 = 50$	$R_4 = 50$
$R_{out} = 100\Omega, 3K\Omega, 10K\Omega$	$R_{out} = 100\Omega, 3K\Omega, 10K\Omega$

Table 2: Component values for the integrating and amplifying stages

4 Shaping

From Figure 12 we notice that the obtained waveform is still not appropriate for the analog-to-digital sampling. The pulse is quite sharp, and we may anticipate that, with a $10ns$ sampling time, there would be non-negligible probability for the maximum amplitude not to be sampled. We also notice that the shaping effect introduced by the time constants, besides bringing the pedestal back to the ground level, also introduces some signal undershooting. This behavior has to be avoided, since it implies an error in the amplitude estimation due to pedestal variations. The solution to both problems has been found by tuning all the time constants involved in the complete circuit (integrating + amplifying stages) and adding an extra RC filter at the output level. The latter acts on the pulse shaping and also reduces noise by attenuating frequencies above the signal spectral composition. The corresponding schematics is shown in Figure 13. We have, as shown in the schematics, four time

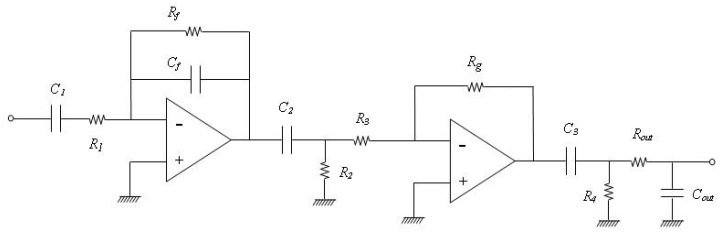

Figure 13: Circuit schematics for a non-inverting configuration.

constants associated to filters that have to be adjusted: the R_fC_f feed-back network which acts on the pedestal level; R_2C_2 and R_4C_3 which act as differentiators; $R_{out}C_{out}$ acting as integrator or low pass filter. These are all first order filters, and their careful combination may avoid the necessity to adopt second or higher order filtering techniques. The differentiating filters control the amount of undershooting, and the integrating filter at the output allows one to fine tune the final waveform shape by varying resistors R_{out}. Simulation results obtained with both operational amplifiers for different R_{out} values are shown in Figures 14 and 15. The list of the other component values used in the simulated implementation is shown in Table 2.

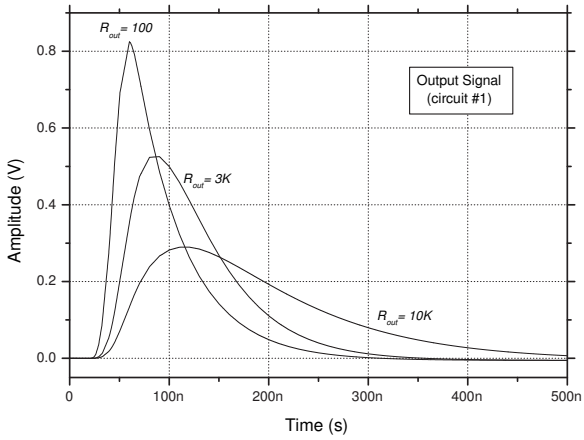

Figure 14: Output waveforms for a pre-amplifier using circuit #1

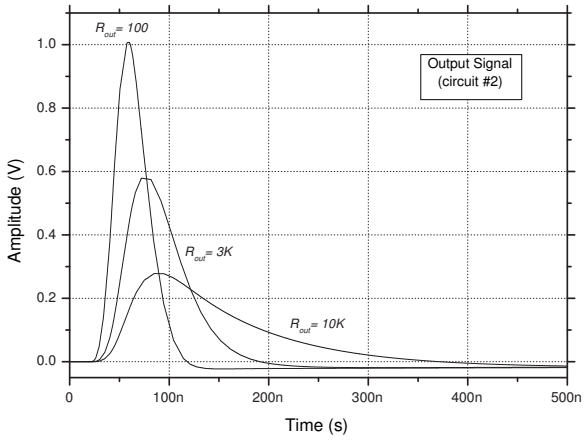

Figure 15: Output waveforms for a pre-amplifier using circuit #2

4.1 Undershoot level

Although the level of undershoot present in the output signal waveform has been well reduced, as compared to Figure 12, it has been found in the simulation results that the time required for the pedestal to be back to the ground level baseline is around $1\mu s$ for circuit #1 and a bit more for circuit #2. As a consequence, if the events count rate is in the range of MHz, there will be a noticeable effect in the amplitude measurement due to undershoot. This is illustrated in Figures 16 and 17. However, the expected count rate in the detector is dominated by cosmic ray events. Given the approximate geometry for the Angra neutrino detector, an estimation of the count rate leads to an average below $5KHz$ [5]. Thus, the average time between consecutive events will be in the range of hundreds of microseconds. In this case, the undershoot level shown in Figures 16 and 17 may be considered as acceptable.

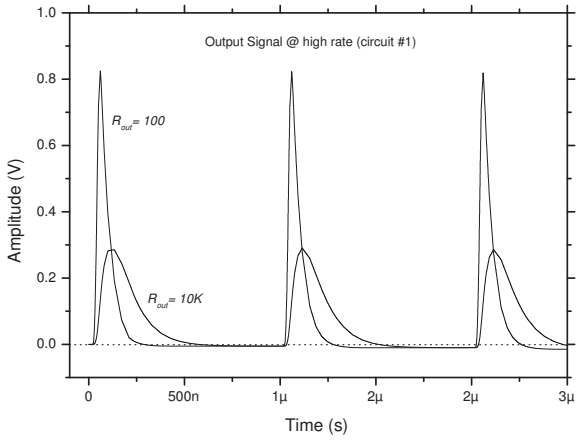

Figure 16: The undershoot effect in a pre-amplifier using circuit #1 for two shaping times.

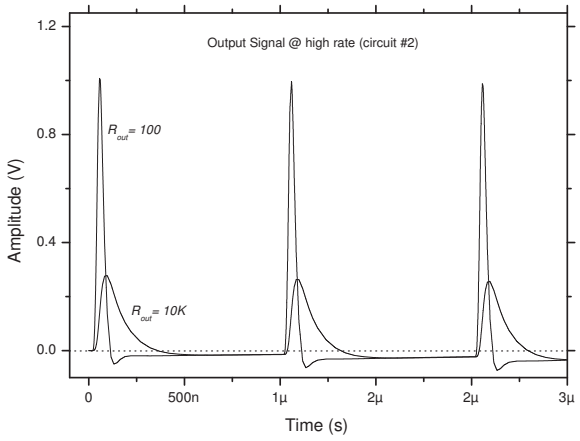

Figure 17: The undershoot effect in a pre-amplifier using circuit #2 for two shaping times.

5 The final circuit

The simulated circuits are simple enough to easily provide the implementation of an inverting or non-inverting mode, by changing the amplifying stage configuration. This change does not have impact on the performance. In addition, it is also possible to introduce a low-pass RC filter in-between the two stages, R being associated to a variable resistor from which we may fine-tune the output waveform. The final circuit schematics for the inverting and the non-inverting circuit configurations are shown in Figure 18. In the final implementation, the $R_{out}C_{out}$ product is fixed to $\approx 20MHz$, so that the output filter mainly limits the bandwidth in order to reduce noise. The circuit's shaping action is concentrated on the filter defined by R_{shape} and C_{shape}. Since R_{shape} is a variable resistor, it determines the shape of the output waveform. The complete circuit is actually a band-pass amplifying filter, with bandwidth defined by R_{shape}. An illustration of the effect of R_{shape} on both the waveform

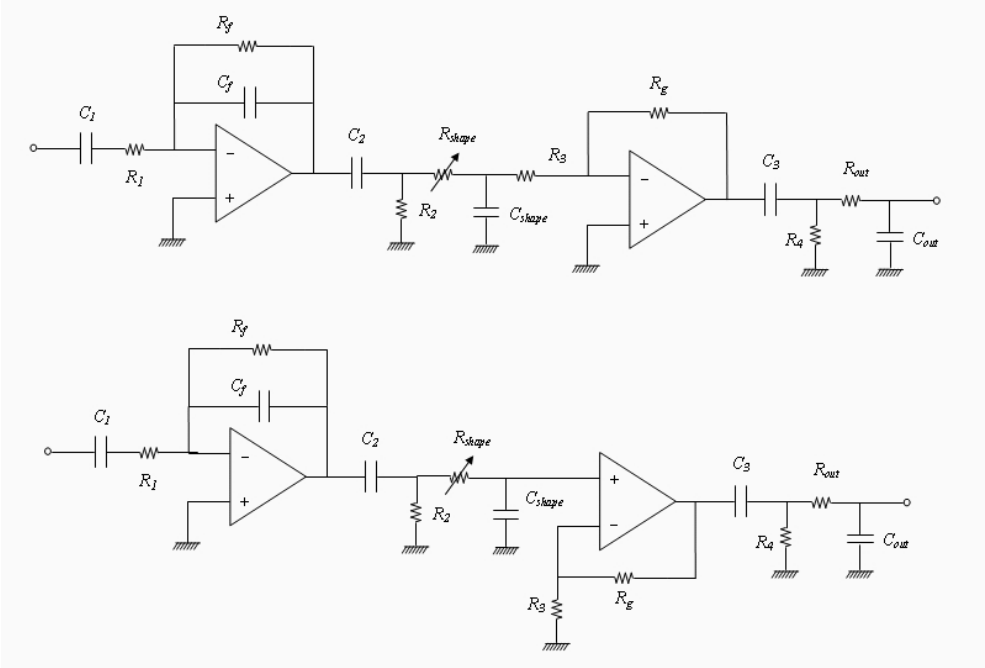

Figure 18: The final schematics for the non-inverting (top) and inverting (bottom) circuit configurations.

(time domain) and the bandpass (frequency domain) is shown in Figure 19, for a pre-amplifier using circuit #1 in the non-inverting version. We therefore obtain the effect of broadening the output pulse, as much as necessary to have it properly sampled by an ADC, by adjusting a variable resistor. In case extra gain or attenuation is required to keep the signal amplitude within the ADC range, the gain may be changed as described above (§ 3.1).

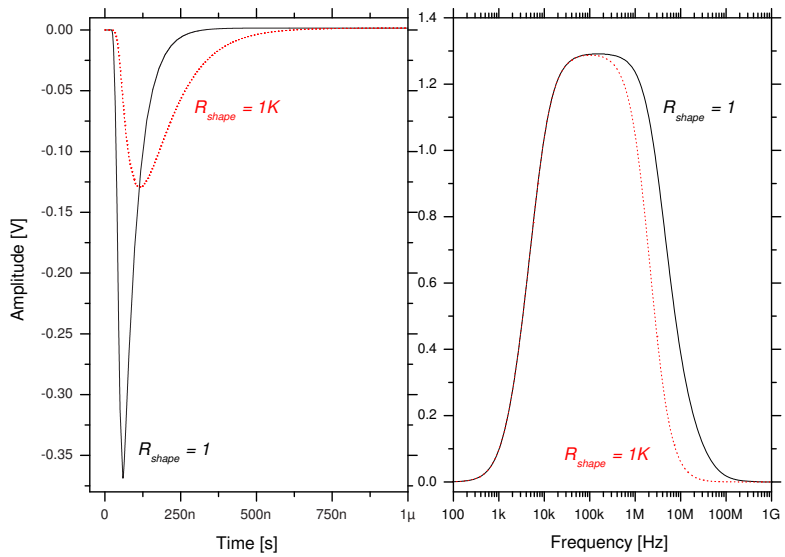

Figure 19: The effect of the shaping resistor on the output waveform (left) and on the bandpass (bottom).

6 Conclusion

In this preliminary study, we have simulated an amplifying and shaping circuit based on two operational amplifiers, converging to a final circuit design that was found to be adequate for the R5912 PMT signals under the expected operating conditions of the Angra anti-neutrino detector. The effective gain and the waveform shape may be tuned by adjusting the value of one circuit component. The circuit is non-inverting, so that the input signal polarity is preserved, but it may be easily made inverting by changing the amplifying stage configuration.

References

[1] J. Anjos et al. Brazilian Journal of Physics. Vol. 36, nro. 4A, 2006.

[2] A. F. Barbosa et al. (unpublished, to be released as an AngraNote).

[3] A. F. Barbosa, E. Kemp, H. P. Lima Junior, A. Vilar. (unpublished, to be released as an AngraNote).

[4] J. Magnin, A. Schilithz. (unpublished, to be released as an AngraNote).

[5] E. Casimiro, F. Simão, J. Anjos. (unpublished, to be released as an AngraNote).